Low Temperature Physics/Fizika Nizkikh Temperatur, 2020, vol. 46, No. 10, pp. 1227–1231

Photoluminescence of Tl_4HgI_6 single crystals

A. I. Kashuba[1], M. V. Solovyov[2], A. V. Franiv[2], B. Andriyevsky[3], T. S. Malyi[2], V. B. Tsyumra[2,4], Ya. A. Zhydachevskyy[4], H. A. Ilchuk[1], and M. V. Fedula[5]

[1]*Lviv Polytechnic National University, Lviv 79646, Ukraine*
E-mail: andriykashuba07@gmail.com

[2]*Ivan Franko National University of Lviv, Lviv 79005, Ukraine*

[3]*Faculty of Electronics and Computer Sciences, Koszalin University of Technology, Koszalin 75-453, Poland*

[4]*Institute of Physics, Polish Academy of Sciences, Warsaw 02-668, Poland*

[5]*Khmelnytskyi National University, Khmelnytskyi 29016, Ukraine*

Received June 9, 2020, published online August 21, 2020

The temperature behavior of Tl_4HgI_6 photoluminescence spectra is presented. The emission spectra are studied in the temperature range between 4.5 and 300 K and in the spectral range 350–650 nm. Two main emission bands at ~ 551 nm and ~ 448 nm are observed corresponding to the emissions of HgI_2 and TlI impurity centers. It is assumed that the low-temperature emission band at ~ 520 nm corresponds to the recombination of the exciton. The luminescence peaks observed in emission spectra in the range between 350 and 410 nm correspond to the phonon repetitions. The excitation spectra of emission bands are measured at 4.5 K and compared with the electron density of states.

Keywords: photoluminescence, emission spectra, decay curve, excitation spectra.

Introduction

The wide bandgap semiconductor crystals attract the attention of researchers due to their wide practical application as the materials for x-ray and γ-ray detectors, for chemical and biomedical industries and others [1, 2]. One of the main issues of material science is the design of radiation sensors, that are efficient at room temperature. Among the known materials (CdTe, CdTe–CdZn, TlBr, MI_2; M = Pb, Hg), the three-component compound Tl_4HgI_6 stands out, because it matches all-important requirements for the radiation detectors [2, 3], the sensor of temperature [4]. The capacitance system of thermoregulation seems to be the simplest way for application Tl_4HgI_6 crystal as a working element of the temperature sensor (see Ref. 4). Most band gaps for semiconductors of interest for radiation detectors fall within the range from 0.7 to about 3 eV [5]. The crystal Tl_4HgI_6 shows the insulating properties with the bandgap $E_g = 2.15$ eV [6]. The thallium component increases the absorption coefficient of the material for x-rays and γ-rays because of its high density, $\rho = 7.15$ g/cm^3 [6, 7], and atomic number, $Z_{Tl} = 81$ ($Z_{Hg} = 80$, $Z_I = 53$). Other parameters of importance for radiation detectors are the electron and hole mobilities along with the propensities for charge trapping or recombination [5].

The compounds containing the ionic-and-covalent bonding are expected to possess the anisotropy of physical properties. It is obvious that the synthesis of novel monocrystalline materials is followed by the research of their basic physical and chemical characteristics: parameters of crystal structure, features of the linear thermal expansion in the temperature ranges of interest, determination of the bandgap, optical characteristics, investigation and interpretation of the photoluminescence spectra. Some results of our previous study of the crystal are presented in [8].

At present time, the studies of optical [6–10], mechanical [4, 11, 12], spectral and energy characteristics are performed for the A_4BX_6 group crystals [13–15] including Tl_4HgI_6 one. The energy band structure studies [9] showed that the direct bandgap corresponds to the G point of the Brillouin zone and the origin of the conduction and valence bands is determined. However, the photoluminescence (PL) studies of A_4BX_6 group crystals are insufficient [1, 3, 10, 16]. The PL investigation of crystals can provide important information about the features of the phonon and exciton spectra, as well as about impurities and defects of the crystal

structure. In the PL spectra of Tl_4HgI_6 crystal [3], the doublet band near 483 and 520 nm and two intensive bands at 565 and 685 nm were identified. The luminescence band at 685 nm is attributed to the impurity levels in the crystal's bandgap [3]. The presence of peak at 565 nm is explained by the recombination of the bound a exciton on the thallium impurity. However, authors of the Ref. 3 have not studied the luminescent excitation spectra and corresponding decay time that could provide useful confirmation for the assumptions proposed.

In the present study, we report the results on the temperature behavior of the PL spectra of Tl_4HgI_6 crystal. The investigation of PL spectra is performed to obtain the information about impurities and structural defects in the crystal.

Experimental

In order to synthesize thallium mercury iodide, we used commercially produced salts of the relevant metal halides. The initial components were taken according to equimolar ratios. Pre-purification of salts was performed by crystallization from melt in quartz ampoules and vacuum sublimation. Tl_4HgI_6 single crystal was grown with a standard Bridgman–Stockburger technique. The details of synthesis conditions are presented in our previous works [7]. The images of the obtained Tl_4HgI_6 compounds are shown in Fig. 1.

PL and PL excitation spectra were measured using a Horiba/Jobin-Yvon Fluorolog-3 spectrofluorometer (with a resolution of 0.2 nm) equipped with a xenon lamp (450 W) and a Hamamatsu R928P photomultiplier. The PL excitation spectra were corrected for the emission spectrum of the lamp. The PL spectra were corrected for the spectral response of the spectrometer system used in our experiments. Finally, low-temperature PL measurements were performed using a continuous-flow liquid-helium cryostat [17].

The theoretical calculations were made using the electron density functional theory (DFT) [9, 10]. For ionic potentials, the ultrasoft Vanderbilt pseudo-potentials were used [18]. To describe the exchange-correlation energy of the electron subsystem, the generalized gradient approximation (GGA) functional with the Perdew–Burke–Ernzerhof (PBE) parameterization [19] was used. The well-known drawback of this approximation is the underestimated bandgap. In this work, to match the absolute values of E_g, the calculated value was corrected by $\Delta E = 0.74$ eV. This does not affect, however, the general trend of the electronic and structural properties, as was confirmed by the previous calculations [9, 10].

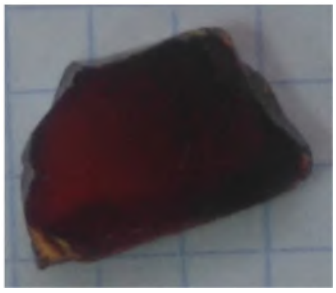

Fig. 1. Typical photo image of studied Tl_4HgI_6 crystal (as-grown).

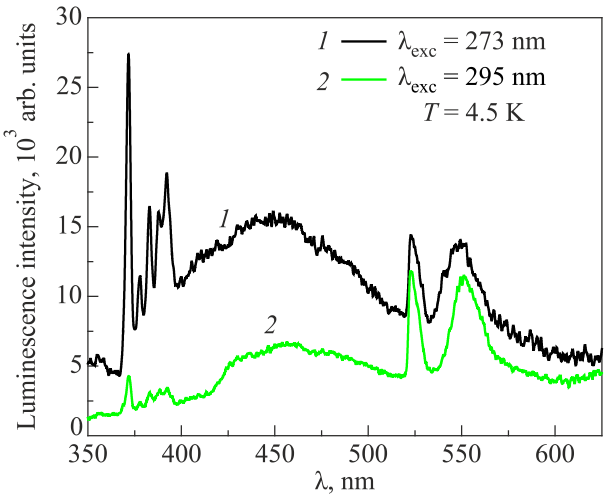

Fig. 2. PL spectra of the Tl_4HgI_6 crystal under excitation wavelengths λ_{exc}= 273 nm and λ_{exc} = 295 nm at temperature 4.5 K.

Results and discussion

The PL bands detected for Tl_4HgI_6 at 4.5 K and different excitation wavelengths are shown in Fig. 2. At low temperatures, several asymmetric bands are observed in the emission spectrum. The luminescence spectra of Tl_4HgI_6 crystal were analyzed with Gaussian curves. As a result, the emission bands at approximately 372, 378, 383, 388, 392, 448, 520 and 551 nm for Tl_4HgI_6 ($T = 4.5$ K, $\lambda_{exc} = 273$ nm) were estimated. The PL spectra of Tl_4HgI_6 at different temperatures between 4.5 and 300 K are shown in Fig. 3.

The temperature behavior of the optical-absorption edge for crystal Tl_4HgI_6 in the temperature range 4.5–300 K was not measured. Taking into account that the bandgap of Tl_4HgI_6 crystal is 2.082 eV at room temperature [3], we

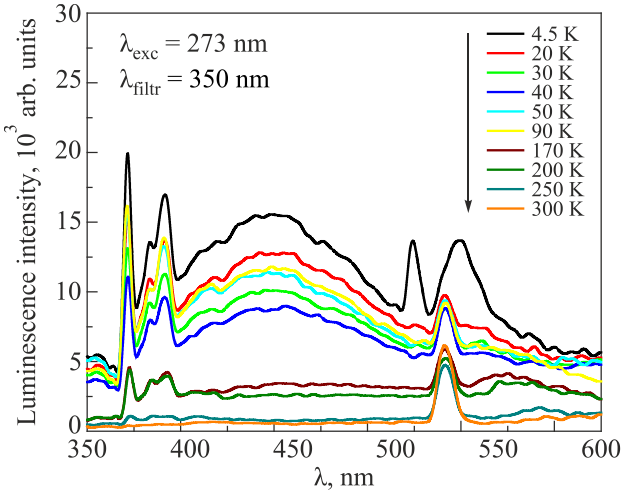

Fig. 3. (Color online) PL spectra of Tl_4HgI_6 obtained at different temperatures.

suppose that the maximum of PL band is shifted about ~ 0.2 eV to the higher energies range [1]. Such difference between the position of the observed PL band and the value of bandgap corresponds to the Stokes shift.

The appearance of the bands near 448 and 551 nm can be related to the shift of the fundamental absorption edge [1, 16]. For the A_4BX_6 group crystals, such a phenomenon is observed quite often [1, 10]. Although the nature of the bands near 448 and 551 nm is not quite clear at present, and it is probably formed by deeply localized states. The PL band at 551 nm (~ 2.25 eV at 4.5 K) is observed at different temperatures in the range between 4.5 and 300 K. It should be noted that the bandgap of HgI_2 crystal is equal to 2.27 eV [20, 21]. Note also that a similar band centered at about 560 nm has earlier been observed for the pure binary HgI_2 compound [20]. Thus we assume that the considered band at 551 nm can correspond to the HgI_2 impurity. On the other hand, no traces of a similar band at 448 nm (~2.78 eV) has been detected in the mercury iodide crystals [20]. The optical absorption edge of the orthorhombic thallium iodide takes place at the photon energy $h\nu \sim 2.84$ eV [22] and the main PL band appears at 451 nm (2.75 eV [23]). Accounting to the optical absorption edge position mentioned above [1], it can be assumed that the band at 448 nm corresponds to the α-TlI impurity [1, 22]. The phenomenon of TlI impurity is observed quite often [1, 10, 16].

It is evident from Fig. 4 that temperature quenching of the luminescence bands at 448 and 551 nm is accompanied by a shift of their maximum position towards higher photon energies. It is worth mentioning that, in a fairly good approximation, the shifts of the maxima positions E_{max} of the PL bands at 448 and 551 nm depend linearly on the temperature. The slopes of the $E_{max}(T)$ dependences are equal to $2.06 \cdot 10^{-4}$ and $7.46 \cdot 10^{-5}$ eV/K, respectively, for the bands at 448 and 551 nm.

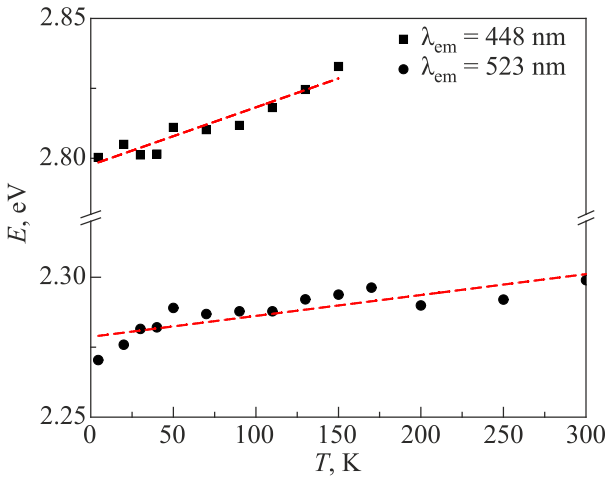

Fig. 4. Temperature dependences of the energy positions E of PL bands maxima at 448 nm and 551 nm (see Fig. 3) measured for Tl_4HgI_6. Lines (- - -) correspond to the linear fits.

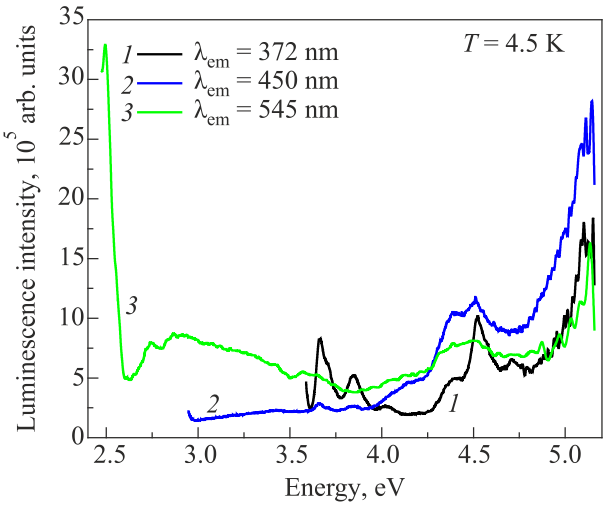

Fig. 5. PL excitation spectra for Tl_4HgI_6 as measured at 4.5 K and different emission wavelengths indicated in the legend.

The observed bands near 392, 388, 383, 378, and 372 nm (Fig. 3) can be attributed to HgI_2 lattice vibrations [24, 25] because the energy shifts between these bands ($\Delta E \sim 33$ meV) are close to the phonon repetitions of the energy $2E_{ph}^{(LO)} = 28.4$ meV [20].

The low-temperature excitation spectra for different emission bands 372, 450, and 545 nm are presented in Fig. 5. These spectra are approximated by Gaussian functions. The positions and half-widths of the bands are presented in Table 1. To check the above assumptions and to explain the real nature of luminescing bands (372, 448, and 551 nm), we compared the PL excitation spectra with the density of states (Fig. 6) [26]. The nature of all the bands in the excitation spectra can be explained using part of the density of thallium, mercury, and iodine states. According to Fig. 6, the bands at 448 (2.78 eV) and 551 nm (2.25 eV) in the excitation spectra can be formed by the emission centers in TlI and HgI_2 impurities, respectively. The band at 372 nm (3.33 eV) is assumed to be related to HgI_2 lattice

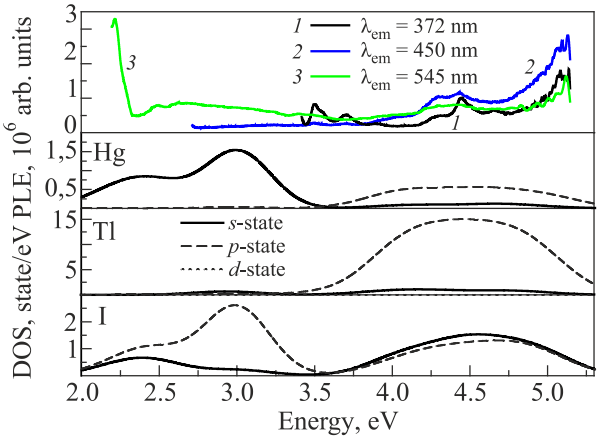

Fig. 6. Density of states compared with the excitation spectra of the Tl_4HgI_6 crystal.

Table 1. Parameters of Gaussian peaks calculated for the PL excitation spectra of Tl_4HgI_6 crystal for the cases of λ_{em}= 372, 450, and 545 nm: FWHM denotes full width of a peak at its half maximum, R^2 is adjusted R-squared value

λ_{em}= 545 nm R^2= 0.981	Peak position, eV	FWHM, meV	Maximum peak intensity I_{max}, 10^5 arb. units
Peak 1	2.49	72.9	23.8
Peak 2	2.64	103.3	9.7
Peak 3	4.02	1002.9	9.0
Peak 4	4.88	459.2	7.6
Peak 5	4.96	63.8	15.8
λ_{em}= 450 nm R^2= 0.991	Peak position, eV	FWHM, meV	Maximum peak intensity I_{max}, 10^5 arb. units
Peak 1	4.25	147.8	2.4
Peak 2	4.45	517.9	8.6
Peak 3	4.51	692.7	15.5
Peak 4	5.28	614.1	27.3
λ_{em}= 372 nm R^2= 0.967	Peak position, eV	FWHM, meV	Maximum peak intensity I_{max}, 10^5 arb. units
Peak 1	3.67	124.4	349.2
Peak 2	4.14	1432.7	25.3
Peak 3	4.38	91.3	1.3
Peak 4	4.53	83.0	4.4
Peak 5	4.93	472.8	9.0
Peak 6	5.09	47.9	3.4

vibrations. Thus, the PL bands at 448 and 551 nm are caused by the internal transitions in the TlI component and HgI_2 compound. We assume that thallium excess may be formed in Tl_4HgI_6 crystal (the same situation is realized in Tl_4CdI_6 crystal [5, 11]). This can be related to the features of the crystal structure and crystal synthesis conditions.

Another intense emission peak is observed at 520 nm. This band is observed only at temperatures below 20 K. We suppose that this band corresponds to exciton emission. The decay luminescence curve of this emission band is presented in Fig. 7. After the kinetic characteristics approximation (Fig. 7) by classic functions for single crystal samples (single-exponential, bi-exponential, expanded exponent, and others [17]), the best convergence of experimental results with the function (1) (R^2 = 0.9978) is obtained:

$$I_{em}(t) \propto A_1 e^{-t/\tau_1} + A_2 e^{-t/\tau_2}, \quad (1)$$

where $A_{1,2}$ denotes constant amplitude factors and $\tau_{1,2}$ characteristic decay times. The two decay components for the emission band at 520 nm are estimated with the characteristic times $\tau_1 = (0.67 \pm 0.01)$ ns and $\tau_2 = (2.66 \pm 0.07)$ ns. The ratio of the corresponding "decay amplitudes" A_i estimated from the fit of Eq. (1) is equal to $A_2/A_1 \approx 3.82$. Since the PL intensity of 520 nm emission band decreases significantly with increasing temperature (see Fig. 3), one can suppose that self-trapped holes are thermally activated and can migrate through the crystal to form a localized bounded exciton emitting at ~ 2.38 eV (see Ref. 3).

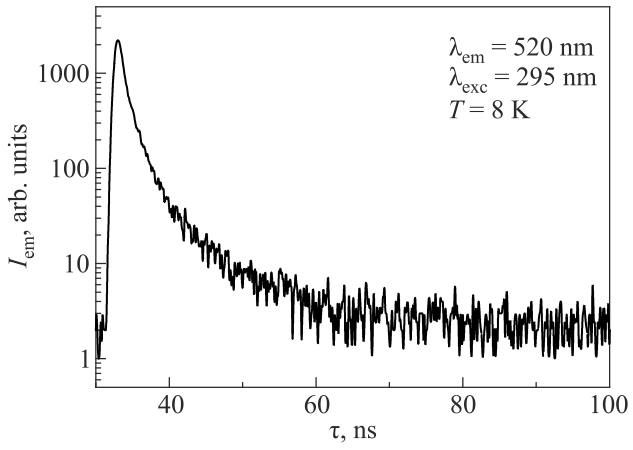

Fig. 7. PL decay curve of Tl_4HgI_6 crystal.

Conclusions

In this work, the PL properties of the Tl_4HgI_6 single crystals were studied. The main bands are observed in the PL spectra at 372, 448, 520, and 551 nm. The strong temperature effect on the PL bands at 448 and 551 nm has been revealed in the range from 4.5 to 300 K. It was found that the temperature quenching of the PL in Tl_4HgI_6 crystal is accompanied with the energy shift of emission bands at 448 and 551 nm towards higher photon energies. The excitation spectra of the luminescence bands at 372, 450, and 545 nm were measured. The measured emission spectra were approximated by Gaussian functions. Based on

the experimental results and DOS calculations, we suppose that the emission band at 448 nm (2.78 eV) belongs to the luminescence in the TlI compound, whereas the bands at 372 (3.33 eV) and 551 nm (2.25 eV) — to the emission of HgI_2. We suppose that the luminescence band at 520 nm corresponds to the exciton emission. The decay curve for the PL band at 520 nm is fitted by two exponential function with two characteristic decay time components $\tau_1 = (0.67 \pm 0.01)$ ns and $\tau_2 = (2.66 \pm 0.07)$ ns. The sharp peaks in the luminescence spectra between 350 and 410 nm can be attributed to the electron-phonon optical transitions.

1. S. Wang, Z. Liu, J. A. Peters, M. Sebastian, S. L. Nguyen, C. D. Malliakas, C. C. Stoumpos, J. Im, A. J. Freeman, B. W. Wessels, and M. G. Kanatzidis, *Cryst. Growth Des.* **14**, 2401 (2014).
2. M. G. Kanatzidis, I. Androulakis, S. Johnses, and S. C. Peter, US Patent No. 8519347 B2 (2013).
3. V. A. Franiv, O. V. Bovgyra, O. S. Kushnir, A. V. Franiv, and O. V. Futey, *Visnyk KhNU* **19**, 65 (2013).
4. V. A. Franiv, O. V. Bovhyra, I. S. Hirnyk, O. S. Kushnir, O. V. Futei, and A. P. Vas'kiv, *Elektron. Informat. Tekhnol.* **3**, 34 (2013).
5. B. D. Milbrath, A.J . Peurrung, M. Bliss, and W. J. Weber, *J. Mater. Res.* **23**, 2561 (2008).
6. M. Piasecki, G. Lakshminarayana, A. O. Fedorchuk, O. S. Kushnir, V. A. Franiv, A. V. Franiv, G. Myronchuk, and K. J. Plucinski, *J. Mater. Sci.: Mater. Electron.* **24**, 1187 (2013).
7. A. I. Kashuba, M. V. Solovyov, T. S. Maliy, I. A. Franiv, O. O. Gomonnai, O. V. Bovgyra, O. V. Futey, A. V. Franiv, and V. B. Stakhura, *J. Phys. Studies* **22**, 2701 (2018).
8. A. Kashuba, M. Solovyov, T. Malyi, I. Semkiv, and A. Franiv, *XI International Scientific and Practical Conference on Electronics and Information Technologies (ELIT-2019)* (2019), p. 272.
9. V. Franiv, O. Bovgyra, O. Kushnir, A. Franiv, and K. J. Plucinski, *Opt. Appl.* **44**, 317 (2014).
10. A. I. Kashuba, T. S. Malyi, M. V. Solovyov, V. B. Stakhura, M. O. Chylii, P. Shchepanskyi, and V. A. Franiv, *Optics and Spectroscopy* **125**, 747 (2018).
11. V. A. Franiv, Z. Czapla, S. Dacko, A. V. Franiv, and O. S. Kushnir, *Ukr. J. Phys.* **59**, 1078 (2014).
12. V. O. Yukhymchuk, V. M. Dzhagan, N. V. Mazur, O. V. Parasyuk, O. Y. Khyzhun, I. V. Luzhnyi, A. M. Yaremko, M. Ya. Valakh, and A. P. Litvinchuk, *J. Raman Spectrosc.* **49**, 1840 (2018).
13. D. V. Badikov, V. V. Badikov, G. M. Kuz'micheva, V. L. Panyutin, V. B. Rybakov, V. I. Chizhikov, G. S. Shevyrdyaeva, and E. S. Shcherbakova, *Inorg. Mater.* **40**, 314 (2004).
14. O. V. Parasyuk, O. Y. Khyzhun, M. Piasecki, I. V. Kityk, G. Lakshminarayana, I. Luzhnyi, P. M. Fochuk, A. O. Fedorchuk, S. I. Levkovets, O. M. Yurchenko, and L. V. Piskach, *Mater. Chem. Phys.* **187**, 156 (2017).
15. A. V. Franiv, O. S. Kushnir, I. S. Girnyk, V. A. Franiv, I. V. Kityk, M. Piasecki, and K. J. Plucinski, *Ukr. J. Phys. Opt.* **14**, 6 (2013).
16. M. Solovyov, A. Kashuba, V. Franiv, A. Franiv, and O. Futey, in: *Proceedings of the IEEE International Young Scientific Forum on Appl. Phys. Engineer*, *YSF-2017* (2017), p. 195.
17. A. I. Kashuba, Ya. A. Zhydachevskyy, I. V. Semkiv, A. V. Franiv, and O. S. Kushnir, *Ukr. J. Phys. Opt.* **19**, 1 (2018).
18. D. Vanderbilt, *Phys. Rev. B* **41**, 789 (1990).
19. J. P. Perdew, K. Burke, and M. Ernzerhof, *Phys. Rev. Lett.* **77**, 3865 (1996).
20. D. Wong and T.E. Schlesinger, *J. Appl. Phys.* **64**, 2049 (1988).
21. Elías López-Cruz, *J. Appl. Phys.* **65**, 874 (1989).
22. A. I. Kashuba, M. Piasecki, O. V. Bovgyra, V. Yo. Stadnyk, P. Demchenko, A. Fedorchuk, A. V. Franiv, and B. Andriyevsky, *Acta Phys. Polon. A* **133**, 68 (2018).
23. Nobuhito Ohno, *J. Lumin.* **119**, 47 (2006).
24. K. Yoshino, M. Sugiyama, D. Maruoka, S. F. Chichibu, H. Komaki, K. Umeda, and T. Ikari, *Physica B* **302–303**, 357 (2001).
25. M. G. Tkachman, T. V. Shubina, V. N. Jmerik, S. V. Ivanov, P. S. Kop'ev, T. Paskova, and B. Monemar, *Semiconductors* **37**, 532 (2003).
26. Thong Leng Lim, M. Nazarov, Tiem Leong Yoon, Lay Chen Low, and M. N. Fauzi Ahmad, *Phys. Scr.* **89**, 095102 (2014).

Фотолюмінесценція монокристалу Tl_4HgI_6

А. І. Кашуба, М. В. Соловйов, А. В. Франів,
Б. Андрієвський, Т. С. Малий, В. Б. Цюмра,
Я. А. Жидачевський, Г. А. Ільчук, М. В. Федула

Подано результати температурної поведінки спектрів фотолюмінесценції Tl_4HgI_6. Дослідження спектрів випромінювання проведено у температурному 4,5–300 К та спектральному 350–650 нм діапазонах. Виявлено дві основні смуги випромінювання ~ 551 та ~ 448 нм, які відповідають випромінюванням домішкових центрів HgI_2 та TlI. Припускається, що низькотемпературна смуга випромінювання ~ 520 нм відповідає рекомбінації екситону. Смуги випромінювання, які спостерігаються в спектрі фотолюмінесценції у діапазоні між 350 та 410 нм, відповідають фононним повторам. Спектри збудження смуг випромінювань вимірюються при 4,5 К та порівнюються з електронною щільністю станів.

Ключові слова: фотолюмінесценція, спектри випромінювання, кінетика загасання люмінесценції, спектри збудження.